CHAPTER 7

FAULT AND DYKE ANALYSIS, MECHANISM OF MAGMA EMPLACEMENT FOR UMKONDO SILLS AND DYKES

7.0 Introduction

Dolerite dykes and sills intrude the Archean basement granites and the Umkondo metasedimentary rocks in eastern Zimbabwe. Some of the dykes are probably related to Umkondo sills as they may have acted as feeders to these sills. Dykes may be used to ascertain the orientations of the principal stresses during their emplacement. Palaeostress analysis can be a useful tool when studying plate motions. Dykes of Umkondo age can give useful information about stresses during Rodinia assembly and Pan African dykes may indicate the stress regime during the breakup of Rodinia and assembly of Gondwana.

In this Chapter the age relationships between faults and dykes in the Chimanimani area are explored. Subsequently, the approaches of Delaney *et al.* (1986) and Jolly and Sanderson (1997) are herein used to perform a palaeostress analysis for dykes that were presumably emplaced along pre-existing fractures in the Chimanimani area.

7.1 Methodology

The azimuths of faults and dykes used for the analyses in this study are to a large extent based on the 1:100000 geological map (Fig. 1.3) of Watson (1969). The map of Watson (1969) was used because an assumption was made that dykes on this map are more likely to be of Umkondo age since some of these intrude rocks of the Umkondo group and some appear to transit into Umkondo sills. Palaeostress analysis on these dykes would constrain the stress regime during the widespread Umkondo magmatism. An effort was made to establish the age relationships between dykes of different trends and between dykes and sills in the field. From Watson's map, it is apparent that faults can curve by up to 20°, and hence it is not straightforward to define the strike of a fault. The following procedure was adopted in order to define a single azimuth.

Each fault/dyke was subdivided into discrete segments. A segment is defined as part of a fault/dyke where change in strike is not in excess of 2°. Dykes are known to consist of segments that are linked by side-steps, horn structures and broken bridges (Nicholson, 1985; Nicholson and Pollard, 1985) and these segments rarely show changes in strike of greater than 45° (Jolly and Sanderson, 1995). The segment analysis was intended to investigate whether curved faults/dykes in fact consisted of segments in discrete orientations. The orientations of segments were directly measured from the geological map and recorded as azimuths ranging from 1° to 180°. The azimuth of an individual fault/dyke is the length-weighted vector mean of the azimuths of the segments that define the fault/dyke. The lengths of faults that extended beyond the maps are minimum values. Thus the length-weighted vector mean azimuth (θ) of *n* segments forming a single dyke/fault of length L ($L = l_1 + l_2 + \text{---} + l_n$) is given as:

$$\theta = \text{Arctan}\ \Sigma l_i X_i / \Sigma l_i Y_i = \text{Arctan}\ [(l_1 X_1 + l_2 X_2 + \text{----} + l_n X_n)/(l_1 Y_1 + l_2 Y_2 + \text{---} + l_n Y_n)],$$

where $X_i = \text{Cos}\ \theta_i$, $Y_i = \text{Sin}\ \theta_i$ and n is the nth segment. θ_i and l_i represent the ith azimuth measurement and length of the ith segment respectively.

The azimuths of the faults/dykes are presented on moving average rose diagrams. The moving average interval was 5°, and the averages were calculated every 1°. The advantage of using moving average rose diagrams is that smoothing is achieved between neighbouring azimuths. The radius of each rose diagram is proportional to the number of total measurements, and the petal length is proportional to the percentage of total measurements that fall within the interval. Fault/dyke sets in this study are defined as adjoining sectors or intervals that have high frequencies and are separated by sectors or intervals that have a very low population or no measurements. Subsets are defined as those regions that have peaks separated by small depressions within each set.

Rose diagrams showing lengths of faults/dykes and their segments with respect to their orientations were plotted by scaling, in which a single entry of a given azimuth represents a fault/dyke length of 1000 m. Thus the azimuth of a fault/dyke of length (*l*

in metres) was entered *n* times, where $n = l/1000$ m. A fault striking 010° with a strike length of 5000 m, for example, implies that 010° was entered 5 times for this single measurement. The frequency of a given azimuth in this case is thus directly proportional to the sum of the strike lengths of faults/dykes having that particular azimuth.

7.2 Results of Fault and Dyke Analysis

The results of fault/dyke analysis are presented on rose diagrams (Figs.7.1 and 7.2) and bar graphs (Fig. 7.3). The faults/dykes are initially classified into 8 cardinal compass directions according to their azimuths (Table 7.1). Faults/dykes trending between northeast and east are classified as set 1 faults/dykes while those trending between south southeast and north northeast are classified as set 2 faults/dykes because adjoining intervals on the rose diagrams do not vary significantly within these ranges (Figs. 7.1 and 7.2). The ranges of the two sets are redefined (Tables 7.2 and 7.3) after trimming azimuths at the extreme ends (Table 7.1) where there are no occurrences of faults/dykes.

Table 7.1. Classification of faults in the Chimanimani area according to their azimuths using 8 cardinal compass directions.

Trend of Dyke/Fault	Azimuth Range	Frequency of Dykes	Frequency of Faults
N	169-180° & 0-11°	21	9
NNE	12-34°	9	3
NE	35-56°	14	12
ENE	57-79°	43	31
E	80-101°	22	9
ESE	102-124°	3	0
SE	125-147°	7	3
SSE	148-168°	26	12

Table 7.2 Classification of faults in the Chimanimani area into two sets and subsets. Most faults in the area have accommodated a dextral (D) strike-slip separation of a few hundreds of metres. S denotes sinistral. Down throw side is predominantly to the south for set 1 faults and to the west for set 2 faults.

Fault set	Fault subset	No. of faults in set	Orientation (°)	Mean length (m)	Shape	Strike-slip separation	Dip-slip separation	Down Throw side
1	1a	41	044 – 078	9100	Curved	D (100-400m)	15 – 70m	South
	1b	9	081 – 099	7000	Curved	S (300) & D (200)	- -	
2	2a	11	148 – 159	5200	Straight	D (100m)	30m	West
	2b	7	165 – 180	4100	Straight	S	30	East
	2b	3	001 – 005	1700	Straight	-	-	
	2d	4	009 – 016	3700	Straight	-	-	

7.3 Faults

Faults and their segments in the area around Chimanimani can be divided into 2 major sets: a dominant set 1 that comprises faults striking between 044º and 092º and set 2 striking between 328º and 016º (Fig. 7.1a). The majority of set 1 faults have accommodated a dextral strike-slip separation and down-throw side is on the south side Table 7.1). Fault segments show smooth trends (Figs. 7.1c and 7.1d) owing to a larger population sample compared to that of individual faults. The fault segments show trends (Fig. 7.1c and 7.1d) that are similar to those of individual faults (Fig. 7.1a and 7.1b). However, there are a few segments that show a south-easterly trend (Fig. 7.1c) that is not shown in the individual fault data (Fig. 7.1a). These possibly represent bends in set 1a faults.

The rose diagrams showing lengths of faults and fault segments (Fig. 7.1b and d) have trends that are similar to those of numbers of faults and their segments (Fig. 7.1a and b). The rose diagrams for fault lengths (Fig. 7.1b and d) show that set 1 faults and fault segments are relatively long and the longest faults and fault segments trend east northeast.

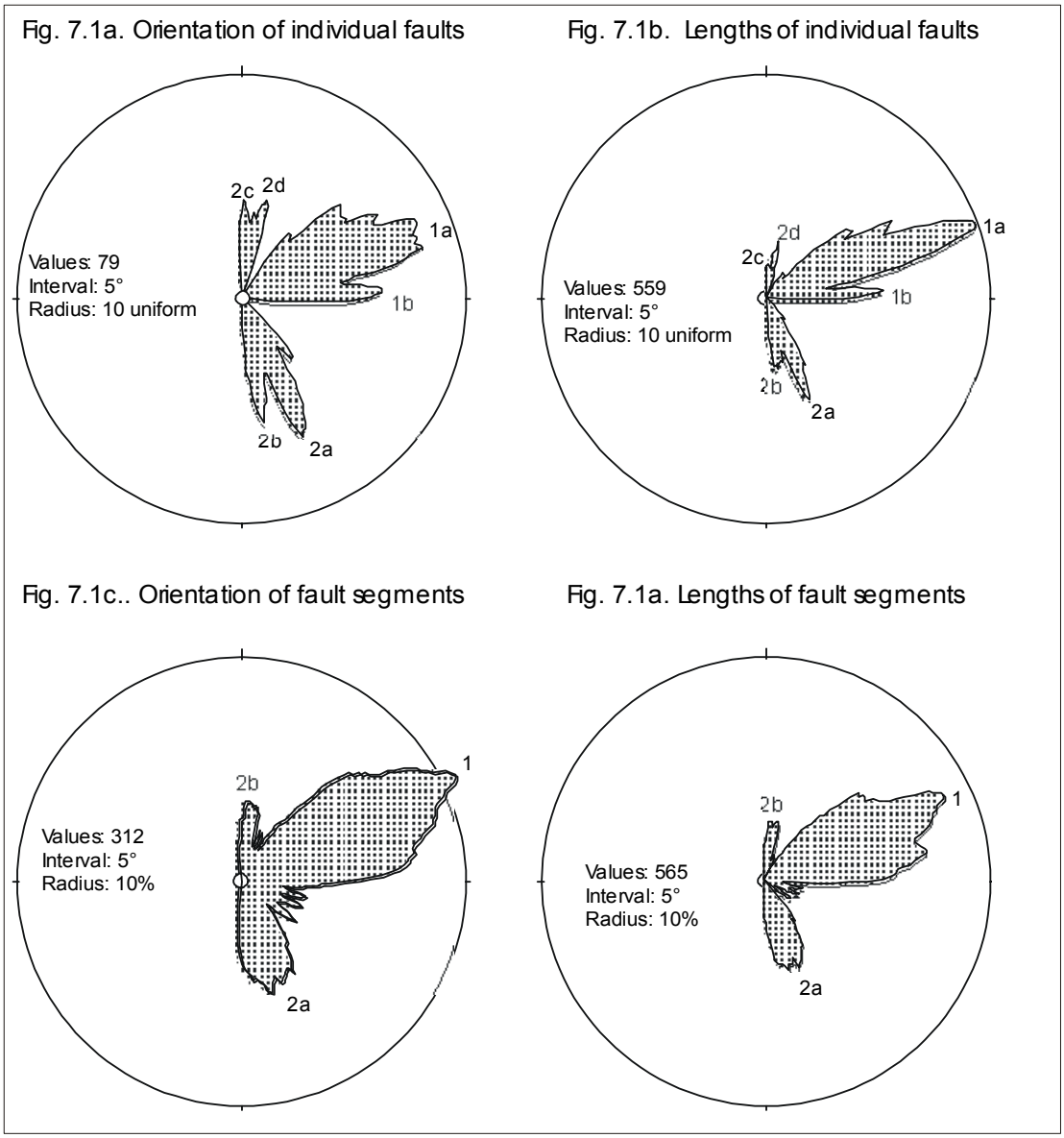

Fig. 7.1. Moving average rose diagrams showing the frequency of the orientation (a) and lengths (b) of individual faults and their segments (c and d) in the area mapped by Watson (1969). The counting interval is 5º, but the interval is shifted in 1º-steps to produce a moving average.

7.3.1 Set 1 Faults

Set 1 faults are curved, concave to the north, sub-vertical to vertical and are relatively long, with an average strike length of about 8.5 km. The majority of the faults are restricted to a dolerite sill, in the western central part of the map, and immediately die out in metasedimentary rocks of the Umkondo Group (Fig. 1.3), possibly due to their low competence. Set 1 faults are subdivided into two subsets (Fig. 7.1a), i.e. subset 1a faults that strike between 044º and 078º and subset 1b faults that strike between 081º

and 092º. The mode and mean azimuths for set 1 faults and set 1 fault segments are east-northeast (Fig. 7.1a and b). Thus set 1 faults and fault segments were mostly propagated in an east northeast/west southwest direction (Fig. 7.1c and 7.1d).

Subset 1a faults are dominant and comprise major faults including the Shinja, Zunguni and Chikwezi-Nyanyadzi faults (Fig. 1.3). The Shinja fault has a strike length of at least 23 km, extending westwards beyond the map (Fig. 1.3), while the Chikwezi-Nyanyadzi fault, to the south, has a strike length of at least 44 km and extends eastwards into Mozambique and westwards beyond the map (Fig. 1.3). The Chikwezi-Nyanyadzi fault has a sinistral strike separation of about 1200 m as evidenced by a displaced sill/granite contact. Displaced contacts and horizons of the Calcareous series and metapelites show that the majority of set 1a faults that show evidence of displacement have vertical separations of 15-70 m, the downthrow mostly being on the south side, and dextral strike separations of 100 to 700 m. A few faults that cut the major sill have dextral strike separations of 100-400 m. The Zunguni fault and other smaller faults of subset 1a, north and south of Outwardbound School (Fig. 1.3; Grid Ref.: 498150; 7814250), have displaced thrusts in the Mozambique facies, mostly, with sinistral strike separations of 200 to 500 m, suggesting that movement across subset 1a faults post-dates the Mozambique orogeny dated at c.550 Ma. Horizons of the Calcareous series (Fig. 1.3) are often truncated by subset 1a faults. A northeast-trending fault, near the southeastern corner of the map (Fig. 1.3), has displaced three north-northwest-trending Mutare dykes suggesting that at least some movement on the fault postdates the emplacement of the dykes. Some subset 1a faults are partly filled with dolerite dykes, and hence the dykes are younger than or contemporaneous with the formation of subset 1a faults.

Most subset 1b faults are relatively short. A notable exception is the major Umvumvumvu fault (Fig. 1.3) and has a strike length of at least 20 km and extends beyond the map into Mozambique. A subset 1b fault with a strike length of about 1.5 km has displaced thrusts of the Mozambique facies with a dextral strike-slip separation of about 200 m which suggests that subset 1b faults either post-date the Mozambique orogeny or represent older faults that were reactivated during the Mozambique orogeny. Most subset 1b faults cut the granite/dolerite sill or

granite/Calcareous series (Watson, 1969) contacts. A subset 1b fault splays from the subset 1a Zunguni fault (Fig. 1.3), just east of Chimanimani town.

7.3.2 Set 2 Faults

Set 2 faults are fairly straight, sub-vertical to vertical and relatively short, with an average strike length of about 4.1 km, and strike between 328º and 016º. Set 2 faults cut rocks of the Umkondo group and do not intersect the dykes. Some of the faults are continuous with dolerite dykes and in places are partly filled with dykes. The set can be subdivided into 4 subsets (Fig. 1a) on the basis of their orientations: subset 2a faults striking 328º to 339º, subset 2b striking 245º to 355º, subset 2c striking 001º to 005º, and subset 2d striking 009º to 016º. There is however no known geological basis for subdividing set 2 faults. Subsets 2c and 2d, comprising of 3 and 4 faults respectively, are uncommon. The mode azimuth for set 2 faults and fault lengths and their segments is north-northwest (Fig. 7.1a and b).

Subset 2a forms the dominant trend in set 2 faults and includes the Nyahodi fault (Fig. 1.3) that has the longest strike length of about 24 km. Evidence of displacement is lacking in most set 2 faults. Subset 2a faults have displaced Calcareous series horizons near the southeastern corner of the map (Fig. 1.3). The displacement shows a dextral strike separation of 100 m and a vertical separation of about 30 m. The down-throw is on the western side. A subset 2b fault has a sinistral strike separation of 100 m and a vertical separation of about 30 m, the down-throw being on the eastern side. Movement across subsets 2c and 2d was too small to be resolved on the map.

7.4 Dolerite Dykes

Dolerite dykes and their segments are fairly straight, sub-vertical to vertical and show two major trends (Table 2) similar to those of faults, i.e. a prevalent set 1 striking between 037° and 095° and set 2 striking between 320° and 027° (Fig. 7.2a and c). The widths of dykes of both sets apparently do not vary significantly along their respective strikes. Set 1 dykes form a dominant trend in granites in the northern part of the map, while rocks of the Umkondo Group host the majority of set 2 dykes. The trends of dyke segments (Figs. 7.1c and d) do not vary significantly from those of

individual dykes (Figs. 7.1a and b). The widths of dykes and their segments do not vary significantly along strike.

Table 7.3. Summary of the results of dyke analysis. Dykes are hosted in granites (G), the upper arkose unit (m3), metapelites (m2), dolerite sills (Dm), quartz-mica schists (m), and quartz vein (Q).

Dyke set	Dyke subset	No. of dykes in set	Orientation (°)	Length range (m)	Mean length (m)	Host rock
1	1a	54	037 – 075	200 – 10900	1600	G, m3, m2, Dm
	1b	24	077 – 095	200 – 20300	3600	G, m3, Dm, Q
2	2a	19	322 – 336	200 – 8800	3500	m3, G, m, Dm
	2b	27	340 – 355	200 – 5200	1300	m3, G, m2, Dm
	2c	4	001-005	300 – 400	300	m3
	2d	9	013 – 027	500 – 10100	4000	m3, G,

7.4.1 Set 1 Dolerite Dykes

Set 1 dykes can be subdivided in to two subsets: subset 1a trending between 037° and 075° and subset 1b trending between 077° and 095°. The modes azimuths for set 1 dyke lengths and their segments are due east (Fig. 7.2 b and d) and vary slightly from that of set 1 faults (Fig. 7.1b) and fault segments (Fig. 7.1d). Set 1 dykes were mainly intrusive into Basement Complex granites (Table 2), where one subset 1b dyke and several subset 1a dykes appear to be possible feeder dykes to sills of unknown ages that intrude Archean basement granites to the north of Wengezi (Fig. 1.3). However, the age relationship between these dykes and the sills remains unclear due to lack of exposure in places where the dykes intersect the sills. Set 1 dykes in granites do not at any point intersect faults, but they do terminate set 2 faults and set 2 dykes. Some set 1 dykes in turn terminate against set 2 dykes. Some set 1 dykes occur along sections of some set 1 faults, which suggest a strong control of dyke emplacement by pre-existing faults.

7.4.2 Set 2 Dolerite Dykes

Set 2 dykes can be subdivided into four subsets: subset 2a trending 322° to 336°, subset 2b trending 340° to 355°, subset 2c trending 001° to 005° and subset 2d trending 013° to 027°. Set 2 dykes exhibit a pattern that mimics that of set 2 faults.

The mode azimuth dyke for set 2 dykes lengths is north-northwest. Subsets 2a and 2b dykes are more commonly hosted in rocks of the Zimbabwe facies and their field relationships with Umkondo sills are not clear. Some subset 2a and 2b dykes that are hosted in Basement granites on the northeastern corner of the map appear to be feeders to sills of unknown ages to the north of Wengezi (Fig. 1.3). Subset 2c dykes are the least common and very short, rarely exceeding 400m, and are restricted to the upper arkose unit of the Zimbabwe facies. Subset 2d dykes intruded either granites or the upper arkose unit and none of these dykes seem to feed any sill. Set 2 dykes, except subset 2c, are continuous with faults.

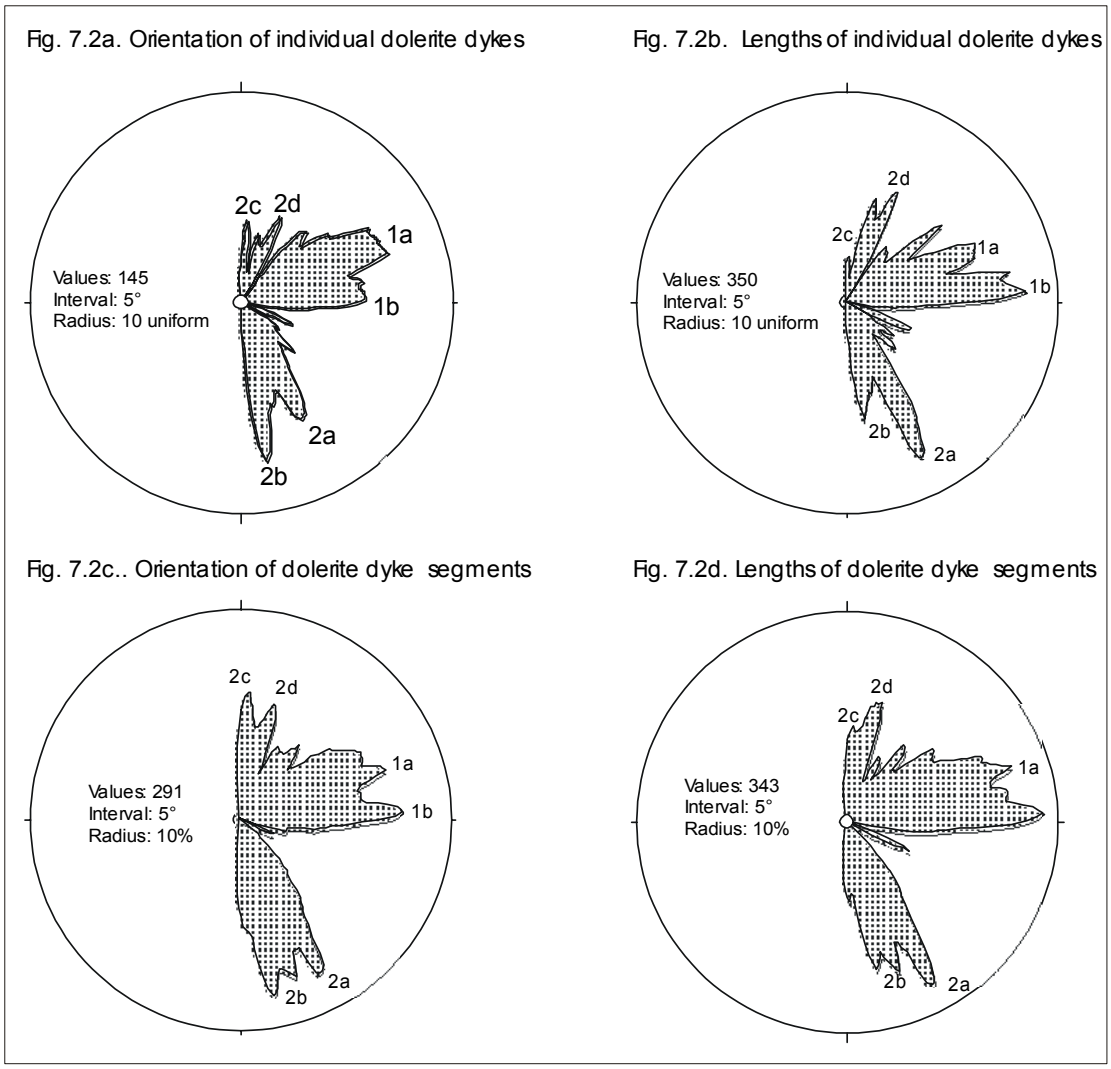

Fig. 7.2. Moving average rose diagrams showing the frequency of the orientation (a) and lengths (b) of individual dolerite dykes and their segments (c and d) in the area mapped by Watson (1969). The counting interval is 5º, but the interval is shifted in 1º-steps to produce a moving average.

7.5 Age Relationships between Faults and Dykes

The age relationships between faults and dykes in the Chimanimani area are problematic because rare displacements across dykes or faults are inconsistent. Some subset 2a dykes have been displaced by a subset 1a fault south of Chimanimani town (Fig. 1.3), which implies that at least some faulting post-dates the dykes. Set 1 faults and set 2 dykes mutually crosscut in places, for example north of Moodies Nek (Grid Ref.: 479700, 7826900) and terminate against each other, for example southwest of Camperdown (Grid Ref.: 473800, 7821100) and west of Moodies Nek (Grid Ref.: 470500, 7825700). Some subset 1a faults have displaced thrusts in the Mozambique facies, north and south of Outwardbound School (Grid Ref.: 498150; 7814250), suggesting that some movement on the faults post-dates the Mozambique orogeny dated at c. 550 Ma. The younger movements on the faults may be due to reactivation after the Pan African orogeny.

Dykes of the two sets may be contemporaneous as suggested by their mutual crosscutting relationships and since set 1 dykes terminate against set 2 dykes and vice-versa (Fig. 1.3). Dykes in both sets form well-defined trends that mimic the trends of the faults in the area. The similarity in trends may reflect that either the dykes were emplaced along pre-existing faults or that the faults were propagated during emplacement of the dykes (Delaney *et al.*, 1986). Dykes may be emplaced along pre-existing fractures that provide planes for the magma to exploit (Currie and Ferguson, 1970; Wilson, 1970; Roberts and Sanderson, 1971; Billings, 1972; Baer *et al.*, 1994; Jolly and Sanderson, 1995). In contrast, magma can propagate a new fracture, which can be intruded by magma, if the magma pressure exceeds the normal stress acting across the fracture plane (Anderson, 1938; 1951; Delaney *et al.* 1986). The opening of such fractures is related to the state of stress at the time of magma emplacement (Delaney *et al.*, 1986). There is, however, a feedback between dyke emplacement and propagation of dyke-parallel fractures that form to accommodate stress resulting from the emplacement of dykes (Delaney *et al.*, 1986; Parfitt and Peacock, 1999).

It is unlikely that the two-dyke sets in the Chimanimani area may have propagated the regional faults in the area. This is because propagation of fractures resulting from

magma emplacement would be demonstrated by the occurrence of prominent dyke-parallel fractures that are closely spaced near the dykes; while fracture-spacing would increase and fractures diminish with distance from the dykes (Delaney *et al.*, 1986), which is not the case in the area. The dyke pattern (Fig. 7.2) mimics that of the faults (Fig.7.1), e.g. the mode azimuths of east northeast and south southwest for set 1 and 2 dykes respectively correspond to those of set 1 and 2 faults (Fig. 7.3). Some set 1 and 2 dykes were emplaced along sections of some faults that cut Umkondo sills (Fig. 1.3). These observations strongly suggest that the formation of these faults was not dependent on magma emplacement, but in fact suggests a structural control on the emplacement of these dykes by pre-existing faults. Moreover, dykes emplaced along faults that cut Umkondo sills clearly point to another magmatic event that post-dates the Umkondo igneous event.

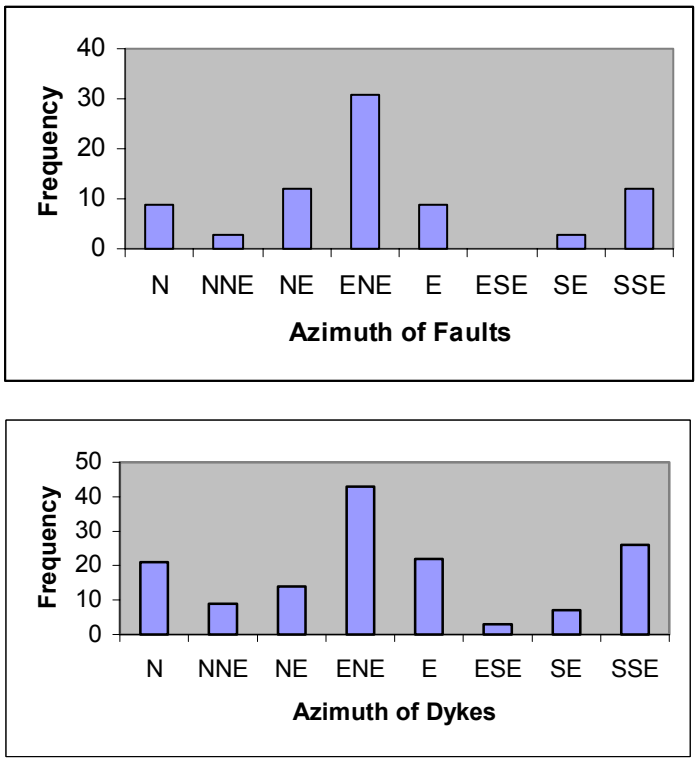

Fig. 7.3. The azimuths of faults/dykes plotted against their frequency show that the trends of dykes mimics that of the faults which strongly suggests that the dykes were emplaced along pre-existing faults.

7.6 Magma Transport Mechanisms

Magma transport is greatly facilitated by fractures (Clemens and Mawer, 1992). Magma is transported within fractures that either become isolated from the magma reservoir or that remain connected to the reservoir (Nakashima, 1993). Transport in the former category is driven by buoyancy of the magma relative to surrounding rocks, and hence the fluid can ascend to the level of neutral buoyancy, or alternatively terminate against a sub-horizontal mechanical anisotropy (Wéertman, 1971, 1980). Magma ascent driven by buoyancy requires that the immediate surrounding rocks be capable of flow and are denser than the magma. Sharp contacts that are chilled and the absence of evidence of recrystallisation in xenoliths and in the country rock near the contact associated with most dykes in eastern Zimbabwe suggest that the mechanism of magma ascent by buoyancy is unlikely. The process is slow due to small density gradients and magma would lose the heat and solidify before reaching the surface (Hogan *et al.*, 1998). Furthermore, the Umkondo basaltic magma is denser than the Archean basement granites, through which the basaltic magma ascended. Thus the buoyancy mechanism does not account for transporting the Umkondo basaltic magma as this transport mechanism would allow the ascent of buoyant felsic magmas while preventing ascent of dense mafic magmas (Tronnes and Brandon, 1992)

Magma ascending within a fracture that remains connected to the reservoir, e.g. a dyke, is driven by the magma driving pressure. In a homogeneous crust, magma can ascend to the level in the crust where the magma driving pressure becomes negligible (Baer and Reches, 1991). Baer and Reches (1991) define magma driving pressure (P_d) as the difference between the sum of the forces that support dyke propagation and remote compressive stress perpendicular to the dyke wall, i.e.

$$P_d = P_h + P_o - P_{vis} - S_h.$$

P_h is the hydrostatic pressure, P_o is the magma chamber overpressure, P_{vis} is the viscous pressure drop, and S_h is the tectonic stress perpendicular to the dyke wall. Compressive stresses are assumed to be positive.

Overpressure of the magma chamber refers to the difference between the pressure within the magma chamber and the confining pressure, and is typically generated by

the tremendous volume increase associated with the bubble nucleation for melts that reach vapour saturation (Hogan *et al.*, 1998). The contribution of the overpressure is therefore negligible in magmas with low volatile contents. The viscous pressure drop is a measure of the viscous resistance to magma flow within a dyke (Baer and Reches, 1991; Hogan *et al.*, 1998). Hydrostatic pressure is the difference between the lithostatic pressure on the top of the magma reservoir, at a source depth D, and the pressure at the top of the column of magma, at some depth Z, as the magma ascends through the crust (Hogan *et al.*, 1998). The hydrostatic pressure can be presented as a function of depth, i.e.

$$(P_h)Z = \rho_c gD - \rho_m g(D - Z),$$

where ρ_c is the integrated density of the crustal column, ρ_m is the integrated density of the magma and g is the acceleration due to gravity.

In a heterogeneous crust, large-scale horizontal anisotropies such as the brittle-ductile transition zone can trap rising magma at deeper crustal levels if the magma driving pressure exceeds the lithostatic load at the depth of anisotropy (Hogan and Gilbert, 1995). The occurrence of Fe-rich tholeiitic flood basalts suggests that dense basaltic magmas rose through relatively less dense continental crust despite their negative buoyancy (Hogan *et al.*, 1998). This implies that large volumes of magma ascended through dykes that remained connected to the magma reservoir so that the magma pressure, to a large extent, determined the emplacement level and final shape of Umkondo magma.

7.7 Crustal Emplacement for Ascending Magma

The final form assumed by a pluton and the emplacement level of magma, is dependent on the magnitude of the magma driving pressure (P_d) relative to the lithostatic stress (S_v), and the availability of potential magma traps (Hogan *et al.* 1998). The emplacement level of magma in the crust partly depends on the magnitude of the magma driving pressure, the presence of sub-horizontal anisotropies such as unconformities, brittle-ductile transition zone; and the magnitude of the lithostatic pressure during ascend. Schematic curves (Fig. 7.4) modified after Hogan *et al.*

(1998) illustrate the relationship between the magma pressure, level of emplacement and the shape of plutons, which are typical of felsic and mafic igneous rocks.

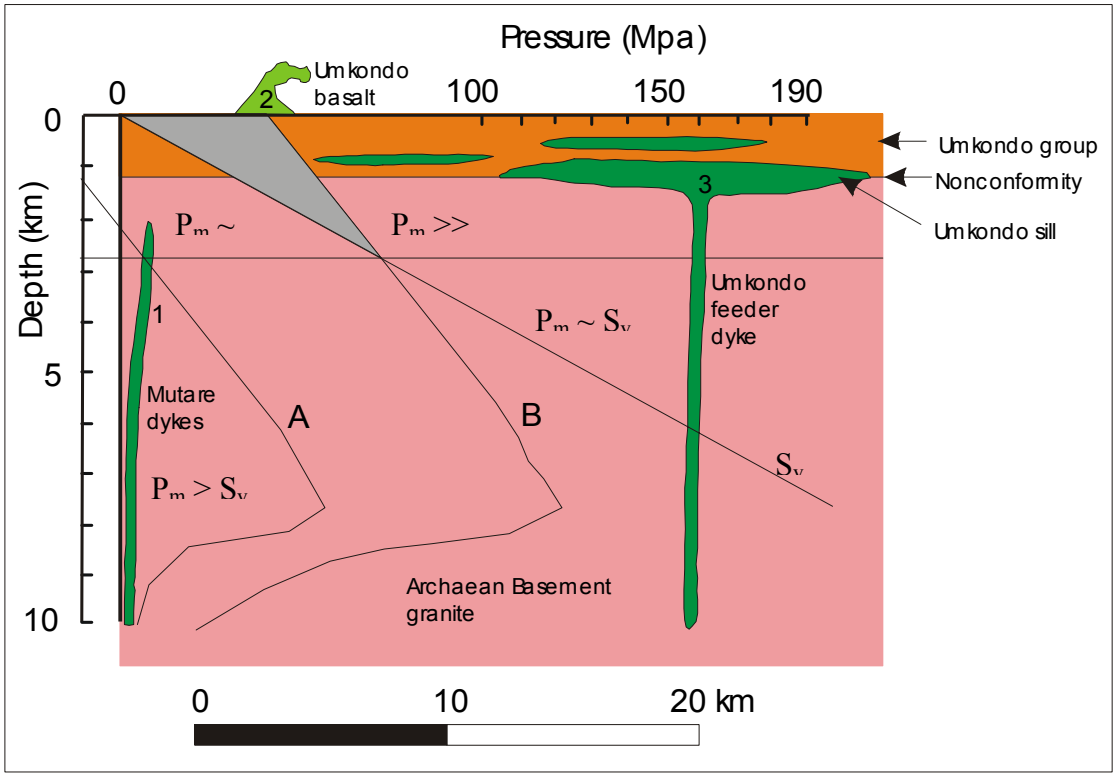

Fig. 7.4 The level of emplacement of Umkondo and lavas and dykes was dependent on the interaction of the magma pressure (P_m) and vertical stress (S_v). Umkondo flood basalts show that the magma driving pressure, at least at times, maintained a positive driving pressure to the surface of the earth. Horizontal anisotropies such as the non-conformity and bedding have facilitated emplacement of Umkondo sills.

7.8 Emplacement Processes: Umkondo Basalts, Dolerite Dykes and Sills

During Umkondo magmatism, the magma, at least at times, maintained a positive driving pressure to the surface of the earth resulting in the eruption of Umkondo flood basalts. The magma pressure required for eruption of the basalts implies that the magma was transported within dykes that maintained connectivity with the magma reservoir (Hogan *et al.*, 1998). Transport of magma was not driven by buoyancy since tholeiitic Umkondo flood basalts are denser than the Archean basement granites, through which the magma ascended. These facts point to the existence of yet undocumented Umkondo dykes that were feeders to the sills and basalts, and it is

possible that some of the Mutare dykes of Wilson *et al.* (1987) could be in fact of Umkondo age.

The anisotropy of the non-conformity and the bedding planes in the Umkondo group to some extent may have facilitated the emplacement of the Umkondo sills (Fig. 7.4). Subhorizontal sheet-like magma chambers are known to form even at low positive driving pressure along pre-existing discontinuities (Chamberlin and Link, 1927; Anderson, 1951; Pollard, 1973; Wéertman, 1980). The presence of Umkondo sills has one of the following two possible implications with regards to the magma driving pressure. Firstly, the occurrence of sills may imply that the magma pressure may have fluctuated so that it did not maintain the positive driving pressure at all times, i.e. when the driving pressure reduced, sills formed and eruptions occurred when the driving pressure rose. An alternative possibility is that magma traps, in the form of anisotropies, operated to create sills in the presence of a continuous positive driving pressure. However, magmas may be emplaced as sills when they reach a level such that the magma pressure is equal to the lithostatic, regardless of any anisotropy.

7.9 Conditions Favourable for Dyke Emplacement along Pre-Existing Joints

Delaney *et al.* (1986) assumed a vertical joint that occupies a portion of a plane $x_1 = 0$ in a 3-coordinate system x_1, x_2 and x_3. The tensile stress and extensional strain are positive; and one regional principal stress is assumed to be vertical. Regional stresses are denoted by σ^r, and σ^c denotes stresses acting on a surface of a joint or dyke. The magnitudes of the principal horizontal stresses are denoted by $-\sigma_1^r = S_h$ and $-\sigma_2^r = S_H$ (Fig. 7.5). Assuming a joint that is long in the vertical x_3 direction relative to its width in the horizontal x_2 direction, Delaney *et al.* (1986) considered the stress acting on a joint in the plane $x_1 = 0$ before it is dilated by an invading magma. The closed joint is assumed to behave like any plane in an unjointed rock, the normal and shear stress components are equal to the regional components, i.e. $\sigma_{11}^c = \sigma_{11}^r$, $\sigma_{12}^c = \sigma_{12}^r$, and $\sigma_{13}^c = \sigma_{13}^r = 0$. The magma imparts a uniform pressure to the joint wall after dilation, $-\sigma_{11}^c = P_m$ and the shear stress is removed, $\sigma_{12}^c = 0$, assuming that pressure gradients due to magma flow is negligible.

For magma to open a pre-existing fracture of orientation θ, the angle between the normal stress and maximum compressive principal stress (Fig 7.5), the magma pressure (P_m) must exceed the normal stress (σ_n) acting on the fracture walls (Delaney *et al.*, 1986), i.e.

$$P_m > \sigma_n. \qquad (1)$$

This can be presented on a Mohr Circle, and for the condition $P_m > \sigma_n$; the stress on the fracture plane must lie in the shaded area (Fig. 7.6).

The normal stress acting on a fracture can be expressed in terms of the fracture orientation (θ), the maximum (S_H) and minimum (S_h) principal stresses, i.e.

$$\sigma_n = (S_H + S_h)/2 + (S_H - S_h)/2 \cos 2\theta. \qquad (2)$$

Delaney *et al.*, 1986, derived the driving stress ratio (R) by substituting equation 2 in equation 1 and rearranging:

$$R = P_m - [(S_H + S_h)/2]/[(S_H - S_h)/2] \geq \cos 2\theta \qquad (3)$$

Equation 3 can be expressed in terms of the mean stress (σ_m) and the maximum shear stress (τ_{max}), i.e.

$$R = (P_m - \sigma_m)/\tau_{max} \geq \cos 2\theta \qquad (4)$$

The driving stress, R, can be derived from the Mohr circle (Fig. 7.6) by considering the triangle AOB. Thus AO can be defined by two equations (Jolly and Sanderson, 1995), i.e.

$$AO = P_m - \sigma_m, \text{ or} \qquad (5)$$

$$AO = \tau_{max} \cos 2\theta, \qquad (6)$$

The two equations (5 and 6) can be combined to give equation 7 below.

$$P_m - \sigma_m \geq \tau_{max} \cos 2\theta. \qquad (7)$$

The following deductions can be made from the Mohr Circle (Jolly and Sanderson, 1997):

- No fractures will open when $R < -1$ ($P_f < S_h$), i.e. the magma pressure is less than the magnitude of the least compressive regional stress and hence is insufficient to dilate a joint of any orientation.
- A limited range of fracture orientations represented by the shaded area (Fig. 7.6) are able to open when $-1 < R < 1$ ($S_h < P_m < S_H$). Fractures to the right of the fluid pressure line (P_m) are unable to dilate.

- Fractures of any orientation can open when R > 1 ($P_m > S_H$), i.e. the magma pressure is greater than the magnitude of the most compressive horizontal regional stress and hence is sufficient to dilate any vertical joint of any orientation (Delaney *et al.*, 1986).

The opening directions of fractures can be determined from the Mohr Circle by considering the triangle FOC in Fig. 7.7. Thus

$$\tan \mu = \tau/(P_m - \sigma_n) = \sin 2\theta/(R - \cos 2\theta), \qquad (8)$$

where τ = FC and CO = $P_m - \sigma_n$. The limiting condition for opening, represented by point B (Fig. 7.6), is $\mu = 90°$; i.e. opening is parallel to the fracture.

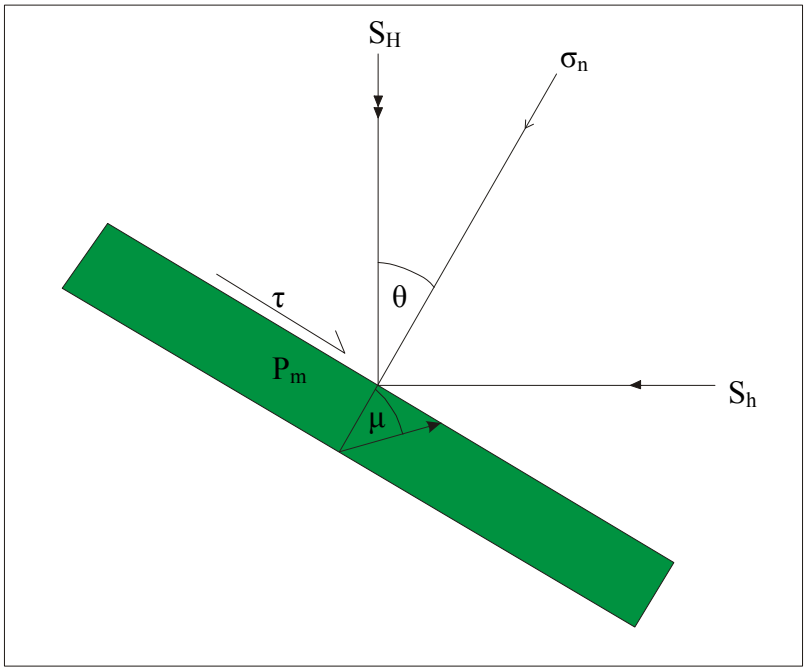

Fig.7.5 The relationship between the normal stress (σ_n), acting on a fracture plane and the fracture orientation (θ), the opening direction (μ) and the maximum (S_H) and minimum (S_h) principal stresses after Jolly and Sanderson (1997).

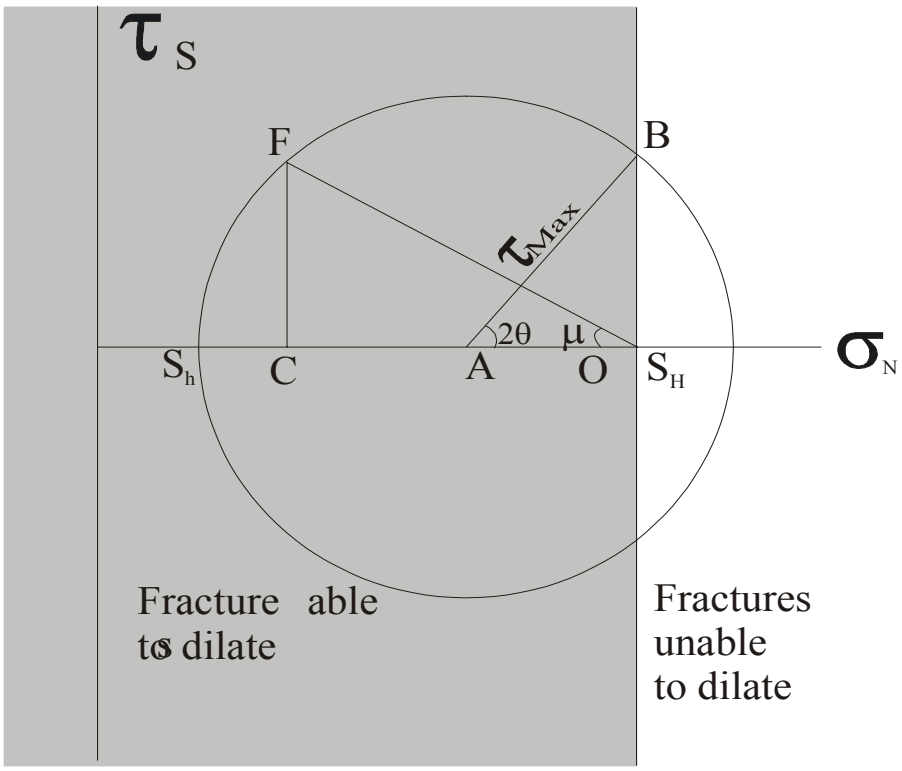

Fig. 7.6. Mohr circle construction, after Jolly and Sanderson (1997), showing the maximum shear stress (τ_{max}), the opening angle of a fracture (μ), and the maximum (S_H) and minimum (S_h) principal stresses.

7.10 Palaeostress Analysis Using Dykes

Two possibilities are considered for palaeostress analyses, firstly for the case assuming that sets 1 and 2 dykes were emplaced during different igneous events and secondly, for the case assuming that the two dyke sets were emplaced contemporaneously (section 7.5). The two sets of dykes were emplaced along pre-existing sub-vertical fractures (section 7.5). Both sets of dykes have a wide range of orientations, which makes the estimate of the palaeostresses difficult.

The orientations of dykes within a dyke swarm are consistent both with one another and with the regional state of stress during time of emplacement (Odé, 1957; Shaw, 1980). Set 1 and 2 dykes dip steeply and are possibly related to extensional or compressional tectonic regimes in which the least principal stress was horizontal, since the dykes are sub-vertical, and orthogonal or at a high angle to the trend of these dykes. If the two dyke sets are assumed to have been emplaced at different times, it may be tempting to use the mode azimuths for the two sets of dykes to deduce the

stresses at the time of emplacement of the dykes. The modes of both dykes sets must not be interpreted to mean that fracture orientations corresponding to these modes were ideally oriented, i.e. were perpendicular to the least compressive stress. This is because the dyke pattern is a function of the pattern of pre-existing faults, i.e. dyke emplacement was structurally controlled (section 7.5). However, the mode azimuth of dykes in a swarm may mean that fractures corresponding to the mode azimuth of the dykes were suitably oriented (Delaney *et al.*, 1986).

The mean azimuths for set 1 and 2 dykes are 70° and 165° respectively. Minimum magma pressure is needed to open fractures that are parallel to σ_1, i.e. the greatest horizontal principal stress (Delaney *et al.*, 1986). Based on the mean azimuths and assuming that set 1 and 2 dykes are not contemporaneous, then the estimated orientations of the least principal stresses were about north northwest-south southeast and east northeast-west southwest during the emplacement of set 1 and set 2 dykes respectively, assuming minimum magma pressure necessary to open each of the fracture sets. Alternatively, it is possible that both sets of dykes are contemporaneous and were opened under a single high magma pressure. The regional principal stresses are not necessarily orthogonal to the pre-existing fracture planes at the time of emplacement (Delaney *et al.*, 1986) and hence it is possible to dilate two fracture sets. In this case the minimum magma pressure necessary to open both sets is given by σ_1, bisecting the smaller angle between the two mean azimuths of the two dyke sets, i.e. about 023°. This follows from the Jolly and Sanderson (1997) stress analysis in the previous section, which shows that for a pair of fractures enclosing any acute angle, the minimum R value will occur for σ_1 in the acute angle between the fractures.

7.11 Discussion and Conclusions

The fault/dyke segments in the Chimanimani area show trends that are similar to those of individual faults/dykes implying that the faults/dykes are made of discrete segments whose azimuths do not vary significantly from those of the mean fault/dyke azimuth. Faults in each of the two sets form well-defined trends, suggesting that the faults in each set formed during a single tectonic regime. Set 1 and 2 faults terminate against each other in places and show mutual crosscutting relationships in places.

These facts suggest that the fault sets are contemporaneous and therefore likely to be conjugate. However, some faults were reactivated after the Mozambique orogeny as evidenced by some set 1 faults that transgress thrusts in the Mozambique facies.

The relative age relationships between set 1 and set 2 dykes and between dykes and sills cannot be established in the field due to lack of exposures where the two-dyke sets intersect or where the dyke sets intersect the sills. Age data for the dykes of both sets is lacking since only one dyke samples yielded any baddeleyite/zircon grains. One set 2 dyke has yielded a U-Pb baddeleyite Pan-African of 724 ± 2.1 Ma (chapter 6). This raises the possibility that at least some of the set 2 dykes are presumably of this Pan African age (724 ± 2.1 Ma) and the stresses related to their emplacement were associated with north-south contractional deformation in the Zambezi belt (Fig. 5.22; section 5.11.2). The emplacement of set 1 dykes was probably related to stresses generated during Rodinia breakup and subsequent east-west collision along the north trending Mozambique belt associated with assembly of Gondwana (Fig. 5.22; section 5.11.2). Alternatively, if the two dyke sets are assumed to be contemporaneous, a north northeast-south southwest oriented maximum principal stress would be required to propagate the two sets simultaneously and would be consistent with contractional structures in the Zambezi belt. In view of the above facts, it is unlikely and an oversimplification to suggest that all the dykes forming the two sets are contemporaneous since available palaeomagnetic, geochemical and geochronological data show that the dykes in the area belong to at least three generations, i.e. Mashonaland, Umkondo and possibly Pan African dykes. A single date from one dyke in eastern Zimbabwe is not sufficient to give a general age of the dykes in eastern Zimbabwe. In fact, the term dyke sets should be used with caution since the dykes within a set may not be contemporaneous.

It is presumed that dykes from each of the two sets were probably emplaced at different ages along parallel fractures that propagated contemporaneously during a single tectonic regime. The dykes in the two sets are inferred to belong to at least three igneous events, i.e. the 1.8 Ga dykes that fed Mashonaland sills, the 1.1 Ga dykes that fed Umkondo sills, and the 0.7 Ga dykes associated with contractional deformation in the Zambezi belt. The assumption of three generations of dykes in eastern Zimbabwe is consistent with geochemical data from these dykes. Ward (2002)

identified three possible magma sources for the Mutare and Guruve dyke swarms of Wilson *et al.* (1987) using major, trace and REE geochemistry and isotopic characteristics. It is possible that dykes belonging to the three generations may have developed craton-wide in Zimbabwe and further work is required to validate this inference. The age relationship between the two dyke sets remains unclear and further precise U-Pb zircon/baddeleyite dating is required. Full confidence in the palaeostress results ascertained using the azimuths of the dyke sets requires more detailed knowledge of the age relationships of the dykes since the dykes are inferred to belong to three magmatic events.

Emplacement of Umkondo sills was probably facilitated by the presence of horizontal anisotropies, i.e. the Archean basement granites/Zimbabwe facies contact and bedding planes in the Zimbabwe facies. Basaltic magma is denser than the host granites and Umkondo Group metasedimentary rocks. Thus buoyancy was not the driving force for magma transport. Magma pressure is the likely driving mechanism that drove the ascent of magma and to a large extent determined the emplacement levels of the magma. The presence of Umkondo basalts shows that the magma pressure may have fluctuated and the magma must have, at least at times, maintained a positive magma pressure to the earth's surface.